GRADUATE AERONAUTICAL LABORATORIES
CALIFORNIA INSTITUTE OF TECHNOLOGY

FM 90-1

Challenges for high-enthalpy gasdynamics research during the 1990's

Plans for the GALCIT T5 Laboratory

H. Hornung and B. Sturtevant

Firestone Flight Sciences Laboratory

Guggenheim Aeronautical Laboratory

Karman Laboratory of Fluid Mechanics and Jet Propulsion

Pasadena

FM 90-1

Challenges for high-enthalpy gasdynamics research during the 1990's

Plans for the GALCIT T5 Laboratory

H. Hornung and B. Sturtevant

Graduate Aeronautical Laboratories
California Institute of Technology
Pasadena, CA 91125

January, 1990

Abstract

Together with Rocketdyne Division of Rockwell Corporation, Caltech has taken an initiative to build a free-piston-driven shock tunnel (known as T5) at its Graduate Aeronautical Laboratories (GALCIT). The facility will provide the means for high enthalpy gas dynamics research and testing, and will cost approximately $3.5M. T5 is expected to be completed in October 1990 and will initially be used by Rocketdyne for tests relating to the National Aerospace Plane (NASP) engine and for fundamental research by GALCIT faculty and graduate students.

This report outlines the motivation for high enthalpy gas dynamics research and the rationale leading to the free-piston driver technique in relation to other flow simulation techniques and to flight tests. It discusses selected important technical and scientific problems demanding fundamental research. The philosophy of the approach to this research, involving the application of modern diagnostic techniques and close coupling with computational fluid dynamics, as well as direct interaction with the aerospace industry, is outlined.

Finally, the current status of the T5 laboratory and its team are briefly described and the financial needs for additional diagnostics and running costs of the research effort are estimated.

This very substantial investment on the part of Rocketdyne and Caltech represents a step that will give the US its first ground facility to produce high density flow at earth orbital enthalpy.

1. Drivers of high-enthalpy gas dynamics research.

When an aerospace vehicle travels through the atmosphere at hypersonic speed U, the specific kinetic energy of the free stream relative to the vehicle is $U^2/2$. At the surface of the body the flow is brought to rest, so that nearly all of its ordered kinetic energy is converted to disordered or thermal energy. If this thermal energy is sufficiently high, a significant fraction of the molecular collisions is of such high energy as to cause molecules to become vibrationally excited and to dissociate, possibly even to ionize. Thus, in the vicinity of the vehicle there exists a flow field in which processes of vibrational excitation and of dissociation (or other chemical processes) are important. They occur at rates which are peculiar to the gas properties and the local conditions. If the rates are very large compared to the rate of flow, the gas is in thermodynamic equilibrium everywhere. Otherwise the additional complication of thermodynamic nonequilibrium must be taken into account. Thus the behavior of the gas is vastly more complex than that of a perfect gas valid at lower speeds.

Such "real gas effects" are clearly of two kinds:

- Because $U^2/2$ is comparable to the specific dissociation energy D, dissociation occurs and the gas can no longer be treated as a perfect gas even if in thermodynamic equilibrium.
- If the rate of dissociation is finite, nonequilibrium effects introduce a time scale that is a property of the gas and the conditions.

To fix ideas, we focus on dissociation, though the same discussion applies throughout to other rate processes.

Those applications in which vehicles travel sufficiently fast to cause chemical reactions to occur in the gas include

- transport to and from space through the earth's atmosphere, orbital transfer
- entry into the atmospheres of the planets or some of their moons, space maneuvers involving aerodynamic braking
- very high speed missiles

Research in high enthalpy gas dynamics has recently been given a strong focus by the establishment of the National Aerospace Plane (NASP) program. The motivation of Rocketdyne to become involved in construction of a high enthalpy facility derives from their present contract relating to the NASP engine. Caltech takes the longer term view appropriate to a university, that the first two items in the above list will continue to increase in importance over the next 20 years. The national need for detailed knowledge of and well-educated specialists in the field is therefore the specific driver for the establishment of a high enthalpy laboratory, at a university such as Caltech, with its tradition of excellence in aerospace research and education.

2. Experimental methods of high-enthalpy gas dynamics.

2.1 Simple scaling laws of real-gas effects.

To focus ideas, it is convenient to consider as a specific problem of high-enthalpy gas dynamics that of the flow over a blunt body, such as a sphere of radius L, in the vicinity of the front stagnation streamline, see Figure 1. In the case of transport through the earth's

atmosphere a typical flow speed for this case is $U = 7\,km/s$. Figure 1 contrasts the case when the gas may be considered to be a perfect diatomic one, with that of the real gas. As may be seen, the temperature profile along the stagnation streamline exhibits very large real-gas effects related both to equilibrium and to nonequilibrium effects. The latter introduce the characteristic length of dissociation l_D related to the dissociation time scale by the flow speed.

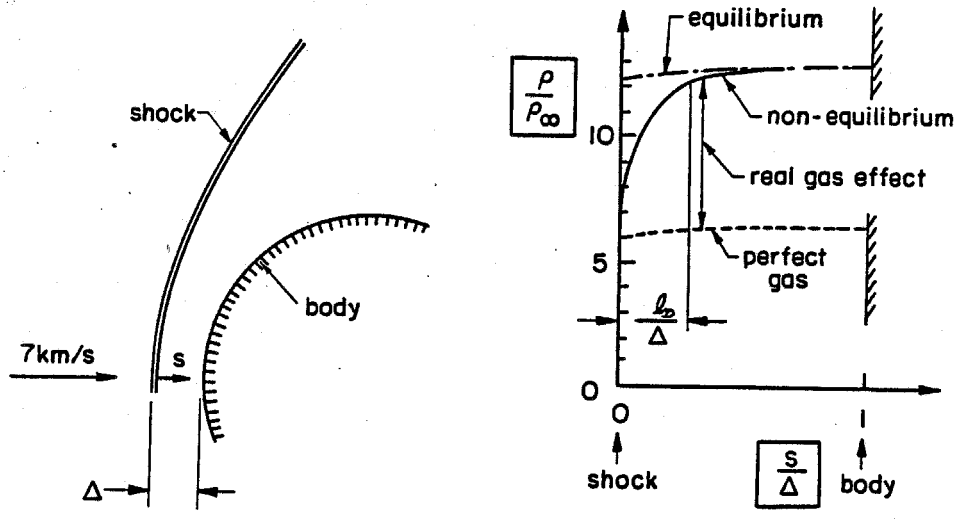

Figure 1 Density profile along the stagnation streamline in a perfect diatomic gas, an equilibrium flow and a nonequilibrium flow. Note the large increase in the density due to real-gas effects and the characteristic length l_D associated with nonequilibrium dissociation.

To generate the same physical effects and flow structure in a test as occur in the real situation of a vehicle flying through the earth's atmosphere at $7\,km/s$, it is necessary that the dimensionless parameters $U^2/2D$ and l_D/L take the same values in the tests as in the real flow. A ground test facility, such as a wind tunnel, therefore needs to provide for the proper duplication specifically of these two, as well as other dimensionless parameters, in order to exhibit comparable real-gas effects. Figure 2 shows just how dramatic the effects of the parameter l_D/L can be in the density field in front of a circular cylinder computed at a specific value of $U^2/2D$, for l_D/L ranging from 0 (equilibrium flow) to ∞ (perfect gas).

The requirement that the flight value of $U^2/2D$ be duplicated in the test facility demands that U be duplicated, since D is a property of the gas, and the many features of the gas properties demand that the same gas be used. D is therefore not free to be chosen. Thus, a flow at a speed of $7\,km/s$ needs to be generated in the laboratory.

The requirement that the flight value l_D/L be duplicated is intimately linked with the need to test at a reduced geometrical scale. Thus, if the real vehicle is scaled down by a factor of 100 for laboratory tests, the dissociation length l_D also has to be scaled down by the same factor. The implications of this requirement become clear in the light of the dependence of l_D

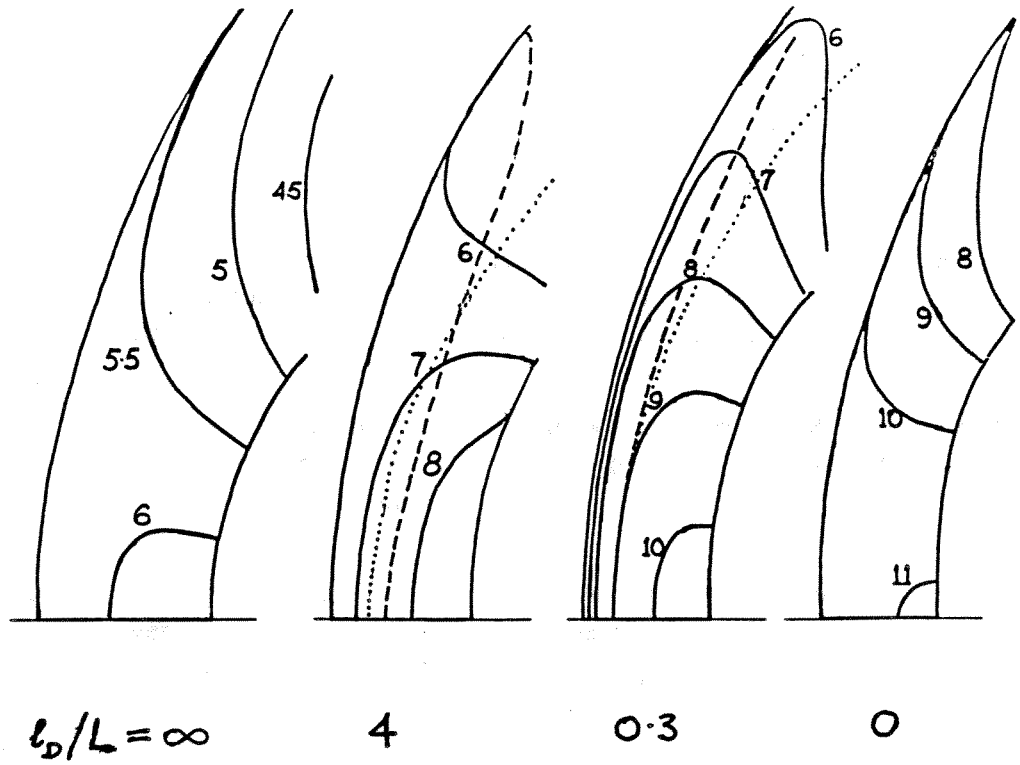

Figure 2 Density field in the shock layer of a circular cylinder in nitrogen flow at $6 km/s$ for different values of the parameter l_D/L. ∞ corresponds to frozen flow (diatomic perfect gas) and 0 corresponds to equilibrium flow. 4 and 0.3 represent relatively slow and fast dissociation. The full lines show lines of constant density indicated in multiples of free-stream density. The dashed and dotted lines are representative temperature and composition contours (from Ref. 1).

on the density ρ. The higher the density, the more frequent are collisions between molecules (other things being equal), and therefore the faster is the dissociation rate. The characteristic length for dissociation is, in fact, inversely proportional to the density or

$$l_D \propto \frac{1}{\rho} .$$

It follows, that for l_D/L to be duplicated, the quantity ρL has to be duplicated.

This type of scaling of the flow is called binary scaling, because it is only for binary chemical reactions such as dissociation that the reaction length is inversely proportional to ρ. If recombination is important, that is for example in flows close to equilibrium, binary scaling fails. The characteristic length for recombination l_R is inversely proportional to the square of the density

$$l_R \propto \frac{1}{\rho^2} .$$

Fortunately, there exists a very large class of important flows in which recombination is so slow as to be irrelevant, and in which it introduces only small scale effects. Nevertheless, it must always be kept in mind that binary scaling is an approximation.

If the quantities U and ρL are both duplicated, the temperature and composition fields will be reproduced in the external flow field of a body. Hence the viscosity field μ, which depends essentially only on the temperature, will also be reproduced. Thus the Reynolds number

$$\mathrm{Re} = \frac{\rho L U}{\mu},$$

which is another important dimensionless parameter, will automatically be reproduced. Exceptions to the applicability of binary scaling occur whenever recombination is important. Examples are boundary layer flow with a catalytic wall and external flows in the atmosphere of Venus.

Two further dimensionless parameters of some importance are the Mach number M and the free stream chemical composition. In some forms of experimental facilities the flight values of these two parameters may not be duplicated correctly. This introduces further problems as will be discussed in section 3.2.

To summarize: For a large class of flows involving high-enthalpy real-gas effects in earth atmospheric maneuvers binary scaling provides a method whereby the essential features of dissociating gas flow may be simulated in the laboratory provided that flight values of U and ρL are duplicated.

2.2 Rationale for simulation facility.

If an air flow at $7 km/s$ is brought to rest at a stagnation point, the temperature reached is approximately 8500K. Conversely, if such an air flow is generated by expanding it through a nozzle from a reservoir at rest, the reservoir temperature has to be approximately 10000K. These are such high temperatures that no material exists to contain the gas for a prolonged period, especially if the pressure in the reservoir is high. It is therefore essential to produce the reservoir conditions for a sufficiently short time to avoid melting and evaporation of the containing material. This limits the testing time, of course, and imposes constraints on the types of experiments that may be performed. The alternative of cooling the walls leads to serious deficiencies in the quality of the nozzle expansion.

A well proven method of heating and compressing a gas at the same time is to pass a shock wave over it and to reflect the shock from a solid surface to heat and compress the gas even more by a second passage. To produce a reservoir at conditions such that the nozzle expansion provides a speed of $7 km/s$, the speed of the primary shock has to be $5 km/s$.

A device of this type, where a shock reflection is used to provide the reservoir for a nozzle expansion to produce a high speed flow, is called a shock tunnel. It consists of a driver tube initially containing driver gas at high pressure and separated from a shock tube containing test gas at low pressure by a strong main diaphragm, and a nozzle and test section initially evacuated and separated from the shock tube by a weak secondary diaphragm. To operate the shock tunnel, the main diaphragm is broken, a shock wave travels through the shock tube, thus heating the test gas. The shock is reflected from the end of the shock tube, where it also breaks the secondary diaphragm. The doubly heated and compressed test gas is thus able to expand and accelerate through the nozzle to the appropriate speed and density. The performance of a simple shock tube, where driver and driven tube have the same cross sectional area may be written down explicitly in the form

$$\frac{p_4}{p_1} = f\left(M_s, \frac{a_4}{a_1}, \gamma_4, \gamma_1\right)$$

where p_4 is the driver gas pressure, p_1 is the test gas pressure, M_s is the shock Mach number, a_4 and a_1 are the driver and test gas speeds of sound and γ_4 and γ_1 are the driver and test gas ratios of specific heat. (This formula does not take into account the real gas effects occurring in the flow after the primary shock and the non-ideal operation of many facilities, but these do not modify the qualitative results of this argument).

In order to discuss the implications of the shock tube formula, it is best to show it in a diagram, see Figure 3. For a particular pair of values of γ_4 and γ_1, Figure 3 shows M_s plotted against p_4/p_1 with a_4/a_1 as parameter. Since the shock speed has to be ~ $5km/s$, this requires M_s to be ~ 15. Figure 3 shows a dashed line at $M_s = 15$, giving a target value to be reached or exceeded. This may clearly be done in two ways: By raising the pressure ratio p_4/p_1, or by raising the speed of sound ratio, or both. The pressure ratio is limited by two requirements. First, the maximum safe pressure is clearly a cost factor and also an operational factor. A reasonable maximum for safe operation in a university environment is 200 MPa. Second, the requirement for ρL duplication dictates increased density for reduced scale. The density is proportional to p_1, so p_1 must not be too small. A reasonable minimum is 10 kPa. Thus, an upper limit on p_4/p_1 is 20000. This is shown as a chain-dotted line in Figure 3. To achieve $M_s \geq 15$ at $p_4/p_1 \leq 20000$, Figure 3 shows that $a_4/a_1 \geq 10$.

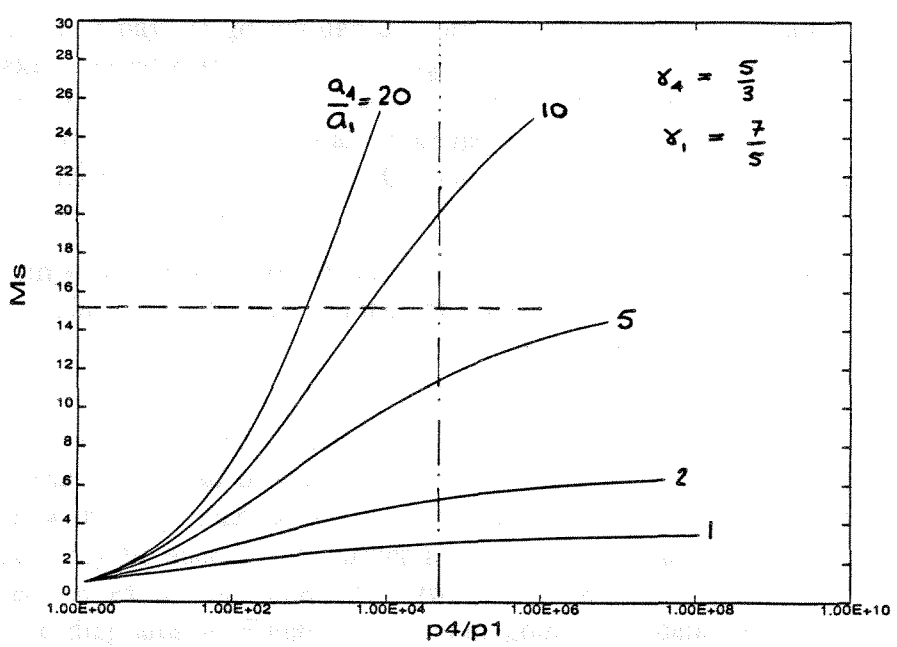

Figure 3 The shock tube formula (see Ref. 2). Safety and flow density restrictions require the pressure ratio p_4/p_1 to lie below 20,000 (chain-dotted line). Enthalpy requirements demand the shock Mach number M_s to reach or exceed 15 (dashed line). For helium driver gas ($\gamma_4 = 5/3$) and air test gas ($\gamma_1 = 7/5$) this dictates that a_4/a_1 be 10 or greater.

It is therefore necessary to produce a high speed of sound in the driver gas. The speed of sound a_4 is related to the temperature T_4 and molecular weight $\mathbf{M}_4$ by

$$a_4^2 = \gamma_4 R T_4 / \mathbf{M}_4 ,$$

where R is the universal gas constant. A light (low $\mathbf{M}_4$) and hot (high T_4) gas is called for. To produce $a_4 \geq 3400\ m/s$ ($a_4/a_1 \geq 10$), in helium ($\mathbf{M}_4 = 4$) requires $T_4 \geq 3500$K. This is also a temperature considerably in excess of the boiling point of stainless steel, so that even the driver gas has to be heated in a transient way.

A clean and repeatable way of heating a gas is to compress it adiabatically by a heavy piston which may be accelerated in a tube, for example by compressed air. If a helium driver gas is heated by a piston compression, a temperature of 4500 K may be achieved with a volume reduction by a factor of 60. This simultaneously raises the pressure by a factor of 1000, so that, to achieve a driver pressure of 150MPa an initial helium pressure, before piston compression, of 150kPa is enough. Clearly, the compression tube has to be long so that the remaining driver gas length at the instant of diaphragm burst is not too small. Also, a number of other requirements including safe piston deceleration complicate the processes occurring during the generation of the shock wave.

A number of shock tunnels using the free-piston driver technique have been built, and several are now under construction. The existing ones known as T1, T2, T3 in Canberra, Australia and T4 at Brisbane, Australia were developed by Stalker from 1961 to 1987. They involved a sequence of scale increases, each of which helped understand the problems associated with size and to find solutions. An important lesson that was learned from this development was that it pays to go through this process of successive upscaling, because even the small steps taken caused many problems. Figure 4 is a brochure of the Australian company WBM-Stalker showing the four existing shock tunnels and three of the facilities presently under construction drawn to the same scale, together with their parameters. A further facility being built by the DLR at Göttingen, W. Germany, known as HEG, lies between T5 and RHYFL in scale (refer to Figure 4).

Many of the important discoveries of high-enthalpy real-gas dynamics were made during the 1970's in the facility T3. A large number of interferometric flow measurements made in that period still provide the best data for computer code calibration at high enthalpy (see section 4).

It is important to discuss briefly alternative methods of producing a fast gas flow with a shock tube as generator. Instead of using a shock reflection to stop the test gas, after heating and accelerating it with the primary shock, and then accelerating it again with a steady nozzle expansion, this gas may be accelerated further by using an unsteady expansion. A device of this type is called an expansion tube. The two principles of operation are compared in corresponding wave diagrams in Figure 5. Without going into detail, the advantages of the expansion tube principle are, that it provides a more accurate reproduction of the free stream composition of the flow (a nozzle expansion is usually not able to fully recombine the gas dissociated by the reflected shock) and that it provides a much more sudden start to the flow (an advantage for heat transfer measurements). One pays for these advantages by smaller size of flow and shorter test time. The facility under construction at GASL (see Figure 4) is a free-piston expansion tube. Without excessive modifications, T5 may be converted to expansion tube operation.

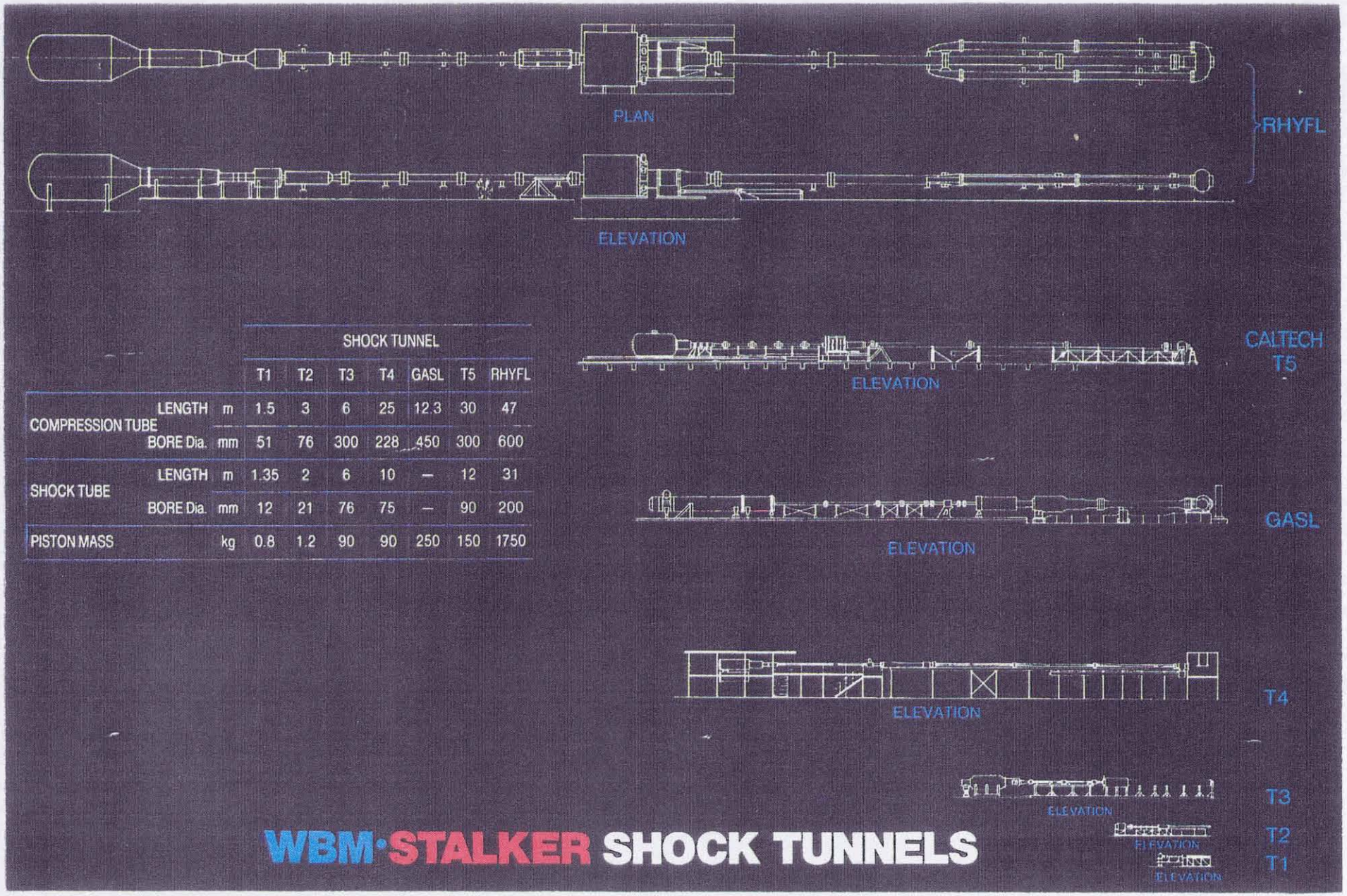

			SHOCK TUNNEL						
			T1	T2	T3	T4	GASL	T5	RHYFL
COMPRESSION TUBE	LENGTH	m	1.5	3	6	25	12.3	30	47
	BORE Dia.	mm	51	76	300	228	450	300	600
SHOCK TUBE	LENGTH	m	1.35	2	6	10	–	12	31
	BORE Dia.	mm	12	21	76	75	–	90	200
PISTON MASS		kg	0.8	1.2	90	90	250	150	1750

Figure 4 Scale increases in some free-piston shock tunnels. The approimate completion dates of these facilities are

T1	T2	T3	T4	T5	GASL	RHYFL
1962	1964	1969	1987	1990	1991	1991

From Ref. 3)

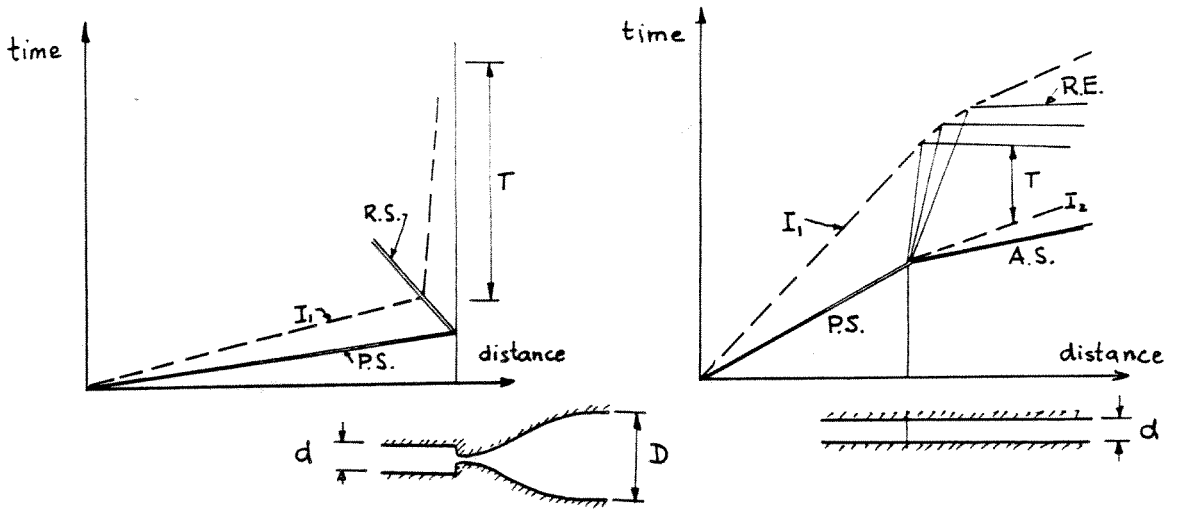

Figure 5 Wave diagrams of reflected shock tunnel (left) and expansion tube (right). Double lines indicate shocks: P. S., R. S. and A. S. denote primary, reflected and accelerated shock. Dashed lines denote interfaces. R. E. is the reflected expansion wave. T indicates the test time. Note that the time scale has been expanded for the expansion tube to show the features better. The expansion tube has a shorter test time and a smaller flow diameter, but gives lower free stream dissociation and more rapid flow start.

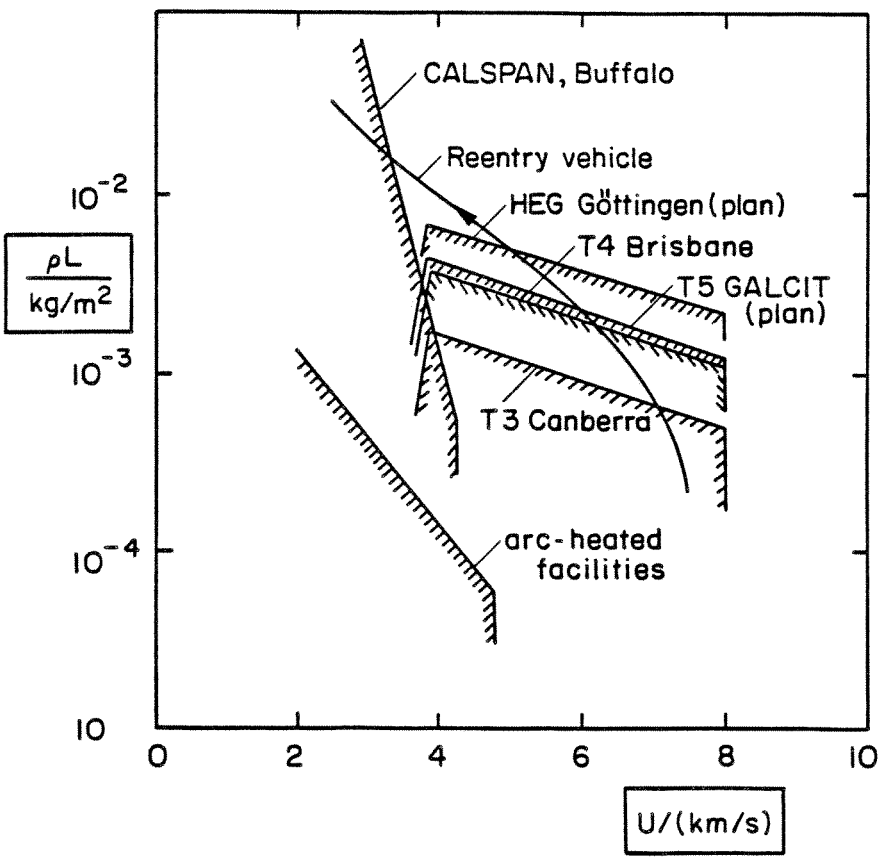

Figure 6 Performance envelope of some facilities for binary scaling of real-gas effects in air, compared with an earth entry trajectory. (From Ref. 4)

Piston facilities depart from ideal shock tube operation, because the effective driver tube is short. This is compensated for to a large part by the fact that the piston continues to move after diaphragm rupture and by the fact that the driver tube area is about 10 times that of the shock tube.

A problem in shock tunnel operation is the termination of the test time through driver gas contamination. The onset of contamination depends critically on the interaction of the reflected shock with the shock tube boundary layer and with the driver/test gas interface.

In order to characterize the performance of different facilities in the context of the high-enthalpy real-gas effects, it is best to show their limits on a plot of ρL against U. This is done in Figure 6 for the free-piston facilities. Development work currently in progress at other laboratories aims to increase the pressure of arc-heated facilities which is presently limited to 20MPa. The projected facility F4 of the ONERA at Toulouse, France aims at a reservoir pressure of 200MPa. So far, the free-piston facilities are the only ones to have achieved the conditions of the critical part of the reentry trajectory which also approximates other aerospace vehicle operations (see Figure 6).

2.3 Flight testing

Clearly, a number of problems of importance may not be studied in a shock tunnel. The short running time eliminates problems involving low frequency geometric adjustments such as are important in engine control. It even eliminates problems associated with large separated flow regions. The large level of disturbances associated with the method of flow generation makes the investigation of transition to turbulence questionable (though both laminar and turbulent flows are reproduced correctly) because transition depends very critically on the level and spectrum of disturbances.

For these reasons it is necessary to complement ground-based experiments with flight tests. Because of their extremely high relative cost it is also necessary, however, to prepare flight tests by extensive ground-based experiments to first eliminate those problems that may be answered cheaply. The approximate ratio of cost per launch for a free flight test to cost per shot in T5 for a model of the same size is 1000, without instrumentation. Since the instrumentation is much more expensive for flight tests, this number is almost doubled.

3. Particular problems of importance

To put this topic into perspective it is helpful to take a brief look at some of the results that have been obtained in T3, because, though these have answered important scientific questions, they have also raised new ones that need to be pursued.

3.1 Selected results from T3 work

One of the first experiments in T3 was designed to examine the phenomenon exhibited by the computation presented in Figure 2, of the effect of dissociative nonequilibrium on the density field of a circular cylinder. The parameter l_D/L was varied in these experiments by changing the cylinder diameter $2L$. Interferometric measurements with infinite fringe width setting (see Figure 7) showed that the dramatic departure of the fringe shapes (equivalent to lines of constant density) from those of perfect gas or equilibrium flow is indeed observed. The change in l_D/L also caused the expected changes. Interesting additional features of these interferograms are that the density rise in the laminar boundary layer is clearly evident and

that, in the case of the 2 inch diameter cylinder a separation line is clearly visible at the rear. A viscous flow simulation was recently performed to compare with these cases and is presented in section 4. These were the first detailed results of strongly dissociating blunt body flows ever measured.

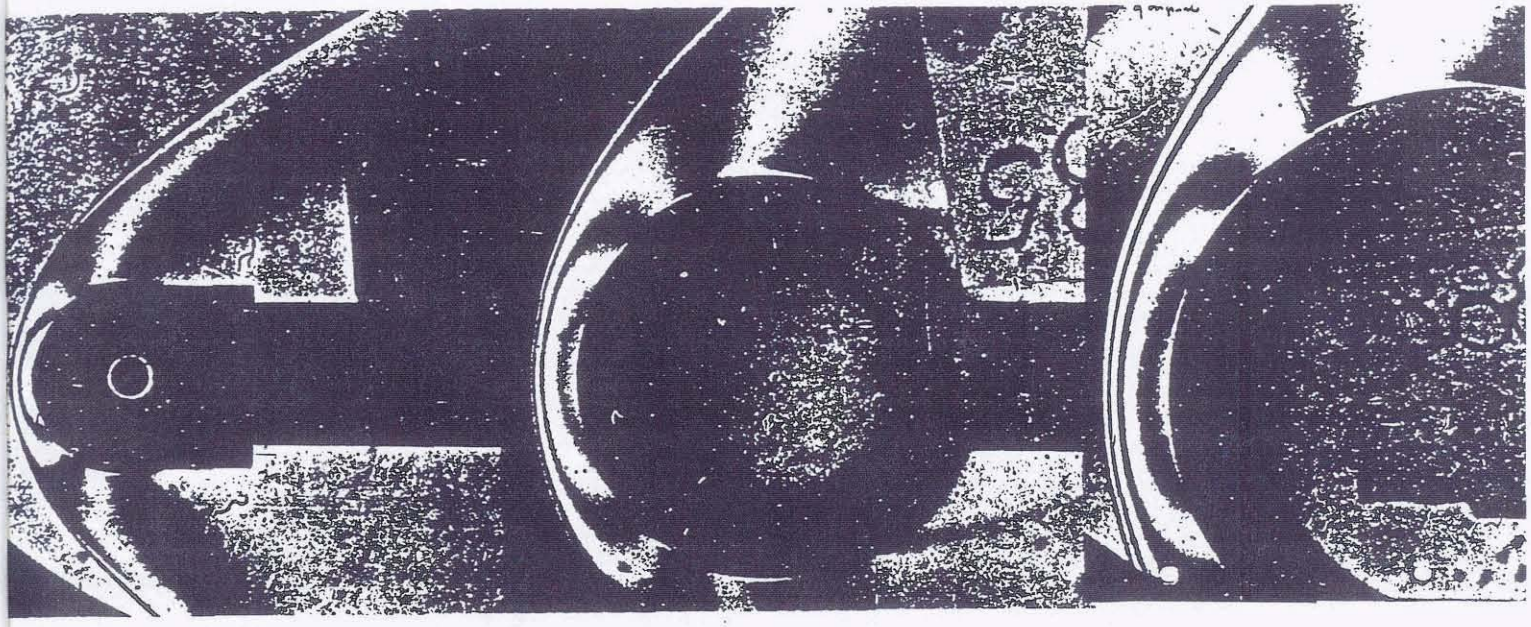

Figure 7 Interferograms of nonequilibrium nitrogen flow at 5.6 km/s over circular cylinders 1, 2 and 4 inches in diameter obtained in T3. The infinite fringe width setting yields fringes that approximate lines of constant density. Comparing these with figure 2, it is clear that strong nonequilibrium dissociation is present and the expected changes due to the variation of l_D/L over a factor of 8 occur. Note the fringe shift due to the density rise in the boundary layer and the separation line in the middle photo. (From Ref. 1)

The understanding of these flows gained through the experiments led to a theoretical investigation of the strongly dissociating region near a curved shock wave. This was based on the asymptotic treatment of the case when $l_D/L \to 0$, i.e., when the thickness of the relaxing layer is small compared with the curvature radius of the shock. This treatment is similar to a boundary layer approach. The results of this study, see Figure 8, led to the very important conclusion that, for a wide range of conditions, the dissociative reaction is stopped because of the cooling resulting from the shock curvature. This effect was called dissociation quenching. A consequence of this effect is that, after the thin reacting layer, the temperature is almost independent of the shock angle β and the density varies as $\sin^2\beta$. This is in contrast to the case of perfect gas flows, where the opposite is the case. The results of this work have very significant value for the designer who can estimate the qualitative effect far downstream of the dissociative flow near the nose of a blunt slender body, in a region where he might wish to place a control surface.

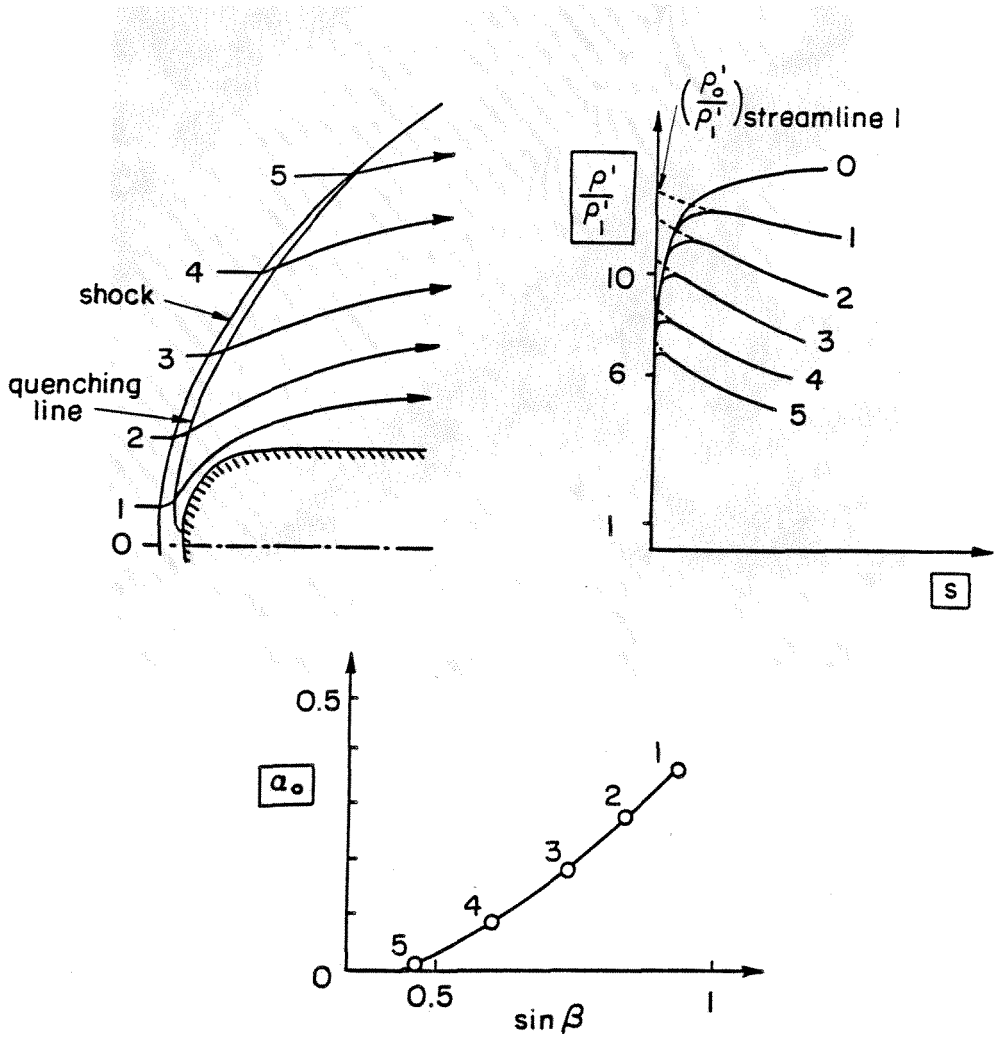

Figure 8 The dissociation quenching effect. Along 5 selected streamlines (top left) that pass through the curved shock and dissociation region before quenching, the top right shows the density profile. The quenched dissociation fraction varies with the shock angle at which the streamline traversed the shock as indicated (bottom). (Ref. 4 and 5)

A further simple flow is that over a wedge, in which the effects of chemical nonequilibrium can be very dramatic. An example of the simple case of flow with an attached shock is shown in Figure 9 in the form of a finite fringe interferogram. The fringe displacement normal to the fringe in the free stream is a measure of the density change. As may be seen, a strong dissociative nonequilibrium effect is evident in the density rise after the shock wave, that occurs over a finite distance l_D before the fringes (and the density) level out again near the body. Again the density rise of the laminar boundary layer may be seen very near the body.

On the basis of a theoretical argument it was predicted in 1977 that the shock detachment distance on a symmetrical wedge would behave very differently in a nonequilibrium flow than in a perfect gas flow. In particular, the detachment distance was predicted to increase very much more gradually from zero. This was indeed observed in both nitrogen and carbon dioxide flows as is shown in Figure 10. The dramatic nonequilibrium real-gas effect exhibited by these results has profound significance for practical vehicle design. Recent computations to compare with these data are presented in section 4.

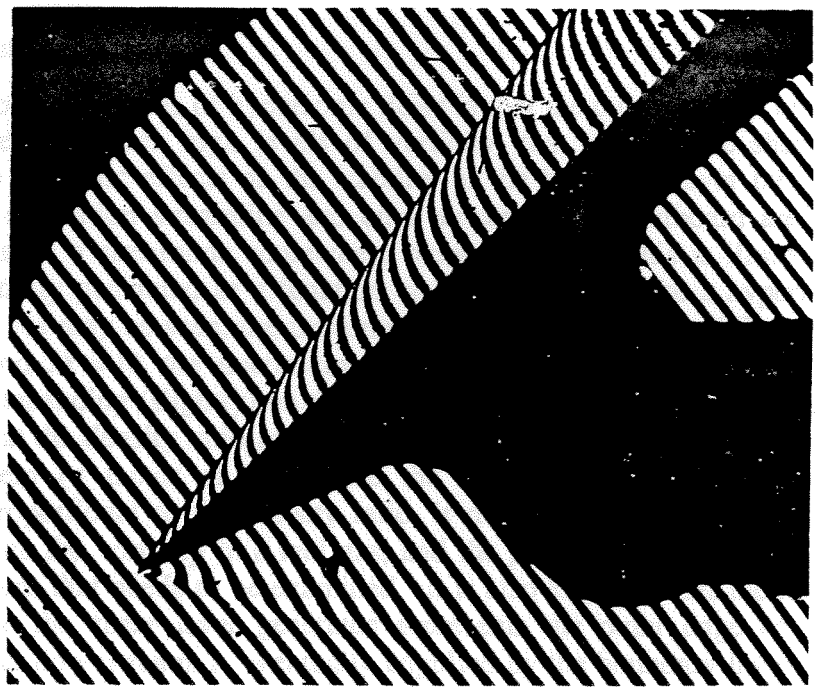

Figure 9 Finite-fringe interferogram of carbon dioxide flow over a wedge at 4.1 km/s. Note rise of fringe shift through the dissociation layer near the shock with subsequent equilibration and rise through the thin boundary layer. (From Ref. 6)

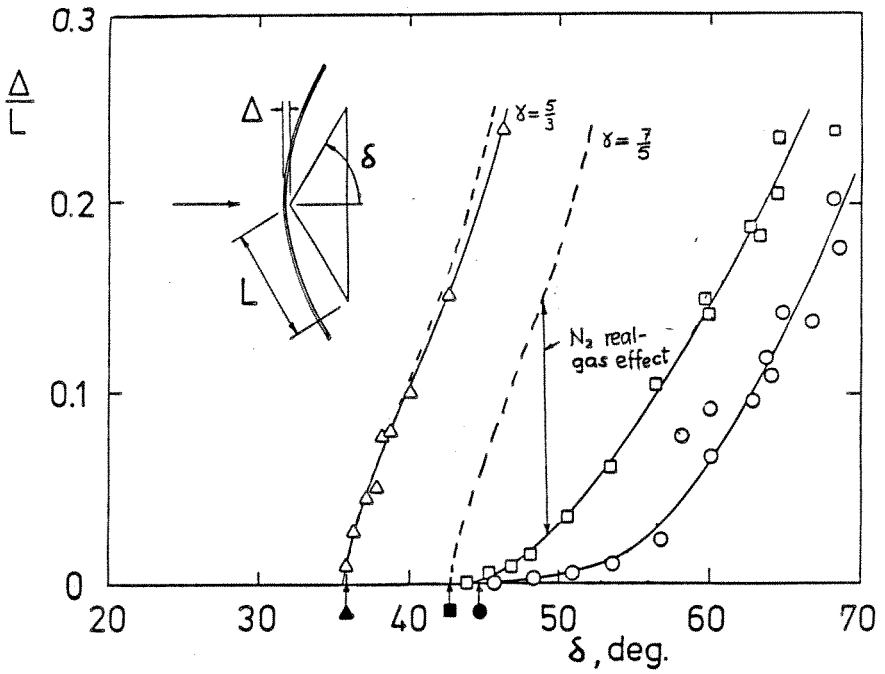

Figure 10 Shock detachment from a wedge. △- perfect gas argon; □- nitrogen, 5.6 km/s; ○- carbon dioxide, 5.1 km/s. Full line: faired through experimental points dashed line: approximate theory for frozen flow. Filled symbols: theoretical detachment angle. (From Ref. 7)

3.2 Important future experiments

One of the special features of hypersonic flows is that the curved shock on the blunt nose of a vehicle can generate such high levels of vorticity, that an unstable shear layer develops, which may have dramatic effects on the stability of the boundary layer far downstream. The vorticity on the stagnation streamline and on a streamline far outboard are both zero, and a maximum occurs on a streamline somewhere between them. This is illustrated in Figure 11 showing the vorticity generated as a function of the shock angle for a hyperbolic shock shape in a perfect gas. As may be seen, the maximum vorticity increases rapidly with Mach number. In fact, at around $M = 10$ the maximum is roughly comparable with the vorticity in the boundary layer, depending (slightly) on the Reynolds number. A very important real-gas effect on this flow is that the density ratio across the thin reacting layer near the shock is dramatically increased by them (≈ factor of 2). Since the vorticity generated at a curved shock is approximately proportional to the density ratio, it may be expected that the shear layer will have roughly twice the vorticity in a real gas, and the phenomenon gains in importance. This is clearly a problem that needs to be examined. It is also known under the name entropy layer swallowing, since the shear layer generated represents the outer edge of a region of high entropy, which, far downstream, is eventually engulfed by the boundary layer.

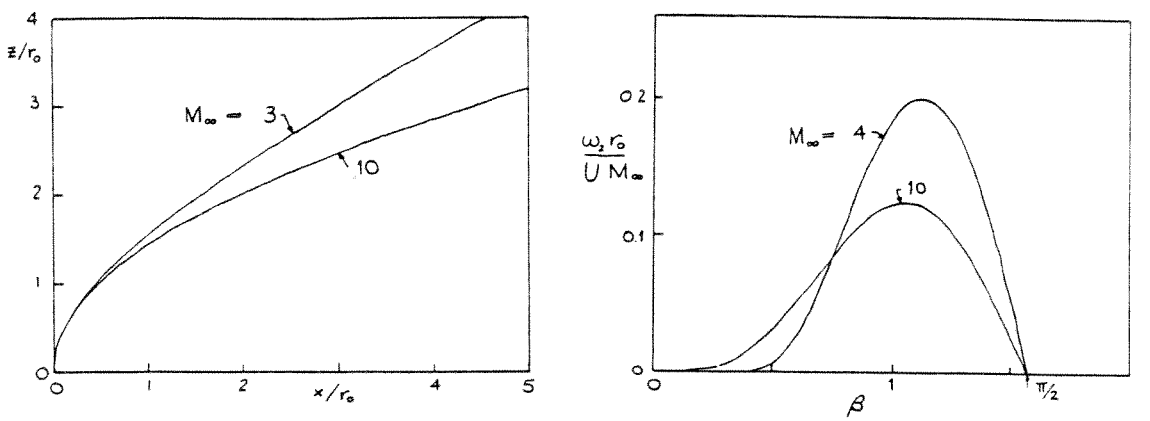

Figure 11 Vorticity produced by the baroclinic torque in a curved hyperbolic shock wave. Left: shock shape, right: normalized distribution of vorticity over the shock angle. (Perfect diatomic gas). Note that the vorticity ω_2 has been divided by the free stream Mach number to be able to plot the two curves on the same diagram. The vorticity maximum increases rapidly with M_∞.

A second important problem is the effect of more complex gas composition (than in the case of nitrogen) on the phenomenon of dissociation quenching after a curved shock. In particular, the intermediate gas NO has a profound effect in the case of the chemistry of air and may cause the relative importance of recombination to increase because of an alternative two-stage path. Such an investigation, like many that are planned, requires intimate coupling of the experiments with a massive computational effort, in which parameters are varied over significant ranges to produce an understanding of the essential and to remove extraneous effects.

Very especially, the higher pressure of T5 vis-a-vis T3 will almost certainly put us in the position of being able to produce a fully developed turbulent boundary layer in high enthalpy flow. We propose to examine the structure of the layer and the energy budget both by optical techniques that integrate along the line of sight (such as interferometry) and by inclined planar

laser-induced fluorescence (PLIF) as well as by wall and profile measurements. Through parameter variations over wide ranges it is expected that qualitative real-gas effects will be discovered and it may be possible to order and classify these. Clearly, this must be an experiment of the exploratory kind that can lead to a well-designed specific experiment only in a second stage.

A very important practical problem of NASP and other vehicles is that of the heat load on the structure. A significant fraction of the effort of the T5 research team must therefore go into the development of satisfactory methods of heat transfer measurement. In a second effort in this direction, the method of thermal protection known as film cooling poses extensive uncertainties and must also be studied in the real-gas environment. Here too, the diagnostic technique PLIF (possibly with seeding of the cooling film) is intended to be applied.

A fifth problem of immediate interest to Rocketdyne for the air-breathing and supersonic combustion engine of NASP is that of turbulent mixing and combustion. To make a fundamental study of this, it is planned to inject hydrogen into the flow with a jet synchronized with the main flow. The technique of achieving this has been determined and partially designed. It involves a second, smaller shock tube to generate the hydrogen jet.

Parallel to these investigations, improvements of the flow quality and duration in T5 should be investigated. Minor reconfigurations of the detail near the ends of the shock tube may be expected to lead to significant improvements and need to be tested.

4. Philosophy of the approach

It is clear that complete simulation in the laboratory of the flow on an aerospace vehicle is not possible. It is also clear, however, that very important discoveries can be made by studying flows that exhibit the main features of the real-gas effects in a fundamental approach. This must be done by getting as close as possible to the real flow by using the proper scaling laws.

The second feature of the approach must be to couple with the experiments a massive computational effort, so that the different computer codes may be calibrated against well-defined experiments with established and specified boundary conditions. Only in this manner can confident extrapolation be made to any real flows.

In both experiments and computations a commonly encountered failing is that no significant parameter variations are made. In the field of real-gas experimentation this parameter variation is of particular importance since the number of possible extraneous effects that need to be eliminated is much greater than in flows in more conventional regimes.

Whenever possible, it is necessary to make measurements carrying not only point information but areal information. For the purpose of resolving unsteady effects such as turbulent structure in shear or boundary layers this is essential. Further, traditional methods, such as schlieren photography or interferometry, which average the information over the line of sight, have fortunately been complemented by techniques such PLIF that resolve spatially along the line of sight. These are eminently more effective methods for comparison with computation.

Finally, it cannot be emphasized too strongly that sensitive indicators of the effects studied must be the ones to measure. To illustrate this principle, consider the blunt body flows of Figure 2 again. A dramatic effect is exhibited by the density field as a result of l_D/L variation. If, instead, the pressure field had been plotted, it would exhibit only very minor quantitative

changes that would certainly be only within the noise of the measurement errors. Hence, density is clearly the variable to measure in this case. In another example shown in Figure 12, the shock configuration can be a sensitive indicator.

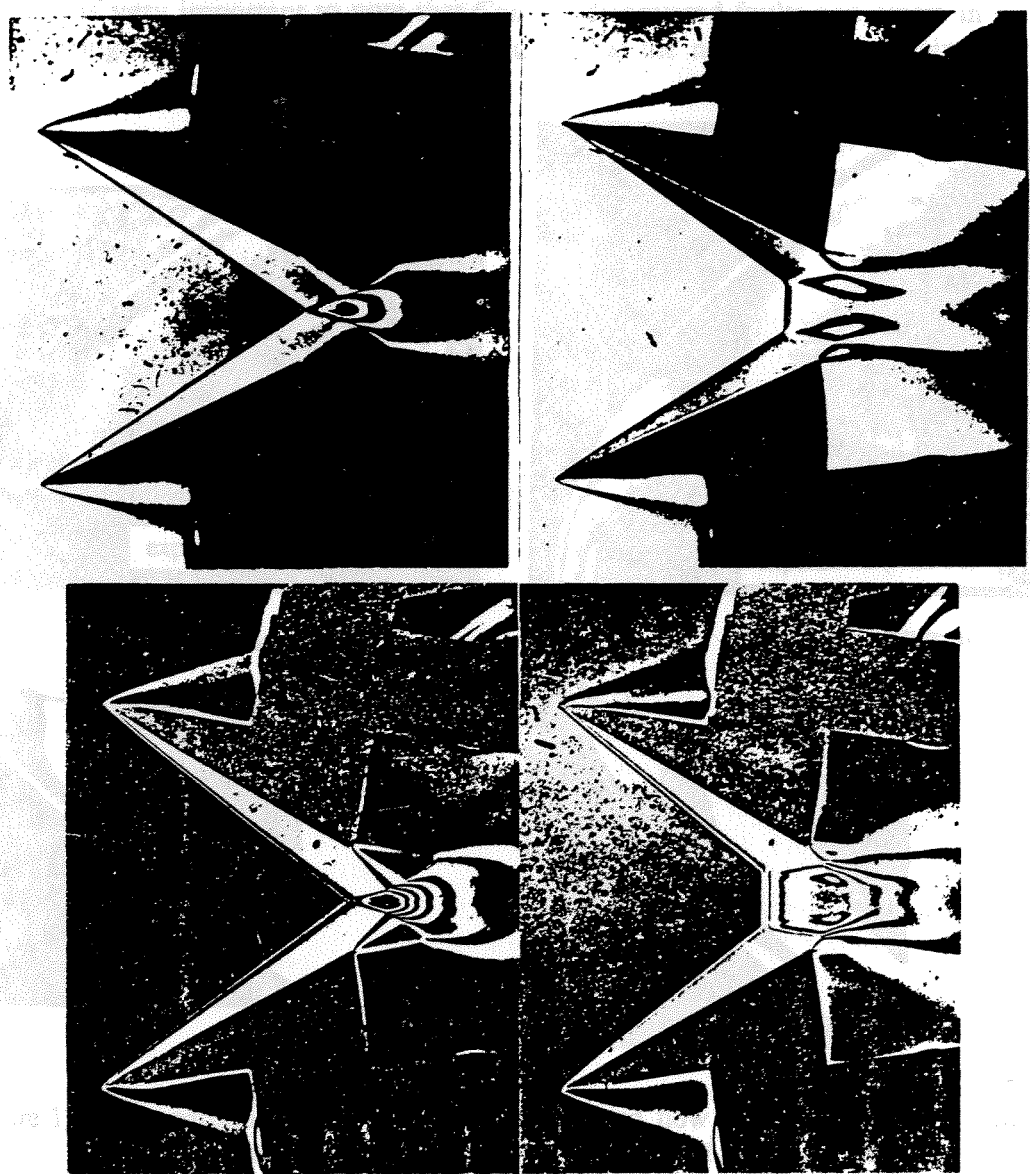

Figure 12 Interferograms of the transition from regular to Mach reflection of shock waves. two wedges are arranged symmetrically to the flow so that the shocks generated reflect from the symmetry plane. On the left, they reflect in the regular and on the right in the Mach reflection mode. Top: nitrogen, bottom: carbon dioxide. In both cases the difference between the wedge angles left to right is less than 0.2 degree. (From Ref. 8)

New developments in instrumentation need to be tried continually, and close contact maintained with leading diagnostics groups. Discussions with Sandia National Laboratories and with Stanford University Mechanical Engineering have helped us in this direction already.

While the approach is to concentrate on fundamental questions, close contact is being maintained with industrial companies in order to keep the information flowing in both directions. Intensive cooperation is clearly already occurring between the T5 team and Rocketdyne, but discussions have also taken place with McDonnell Douglas. To illustrate our

first efforts to couple modern computation with this work, Figure 13 shows comparisons of two of the flows of Figure 7 with computations by Candler. More recently, Candler at our suggestion also computed the shock detachment from a wedge with spectacular results, see Figure 14. It is very important to note that Candler discovered faults and errors in his grid and code only through comparison with experiment, so that the need for the combined approach is evident.

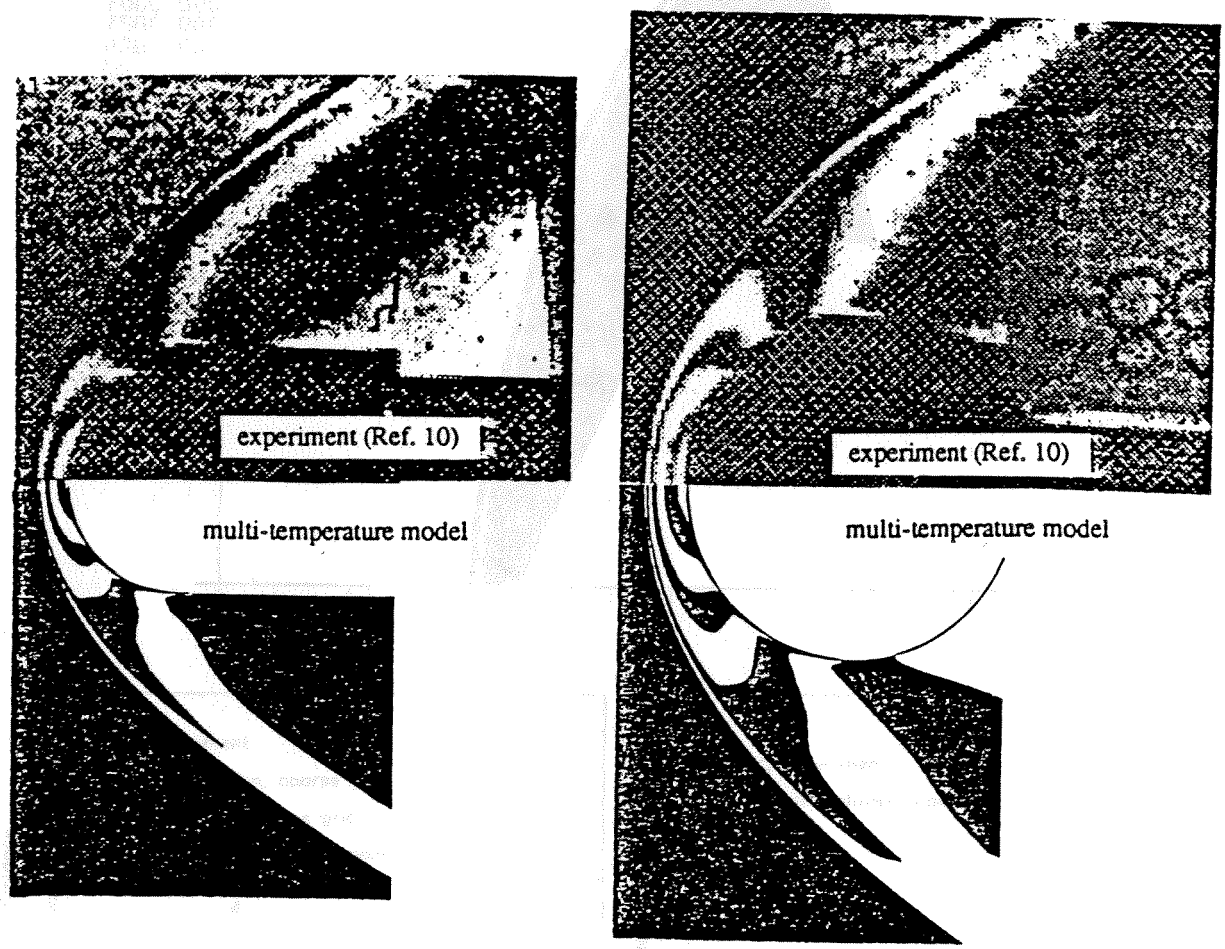

Figure 13 Comparison of experimental and computed flow of nitrogen over a circular cylinder (see also Figure 7) by Candler. In each of the two cases the top half is the experimental interferogram (Figure 7) and the bottom is the corresponding computed one. All the special features of the flow are faithfully reproduced by the computation. (From Ref. 9)

5. Status of the T5 lab and its team (1-30-90)

5.1 Hardware, diagnostics, computer codes

The construction of the new laboratory building on the roof of Guggenheim building including utilities is complete. Part of the roof of the new building has been left open to allow the hardware to be brought up by crane. The roof location has been chosen because this was the only place at GALCIT where a straight 200 ft length could be found. Figure 15 shows a photograph of the laboratory.

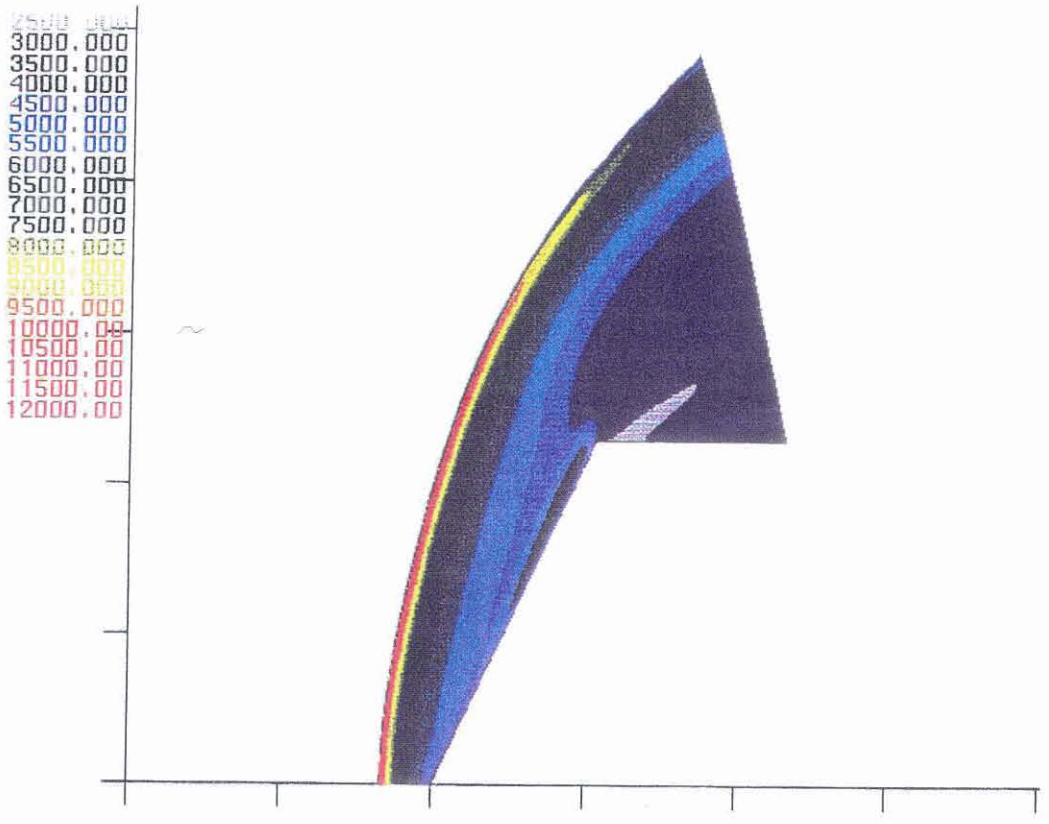

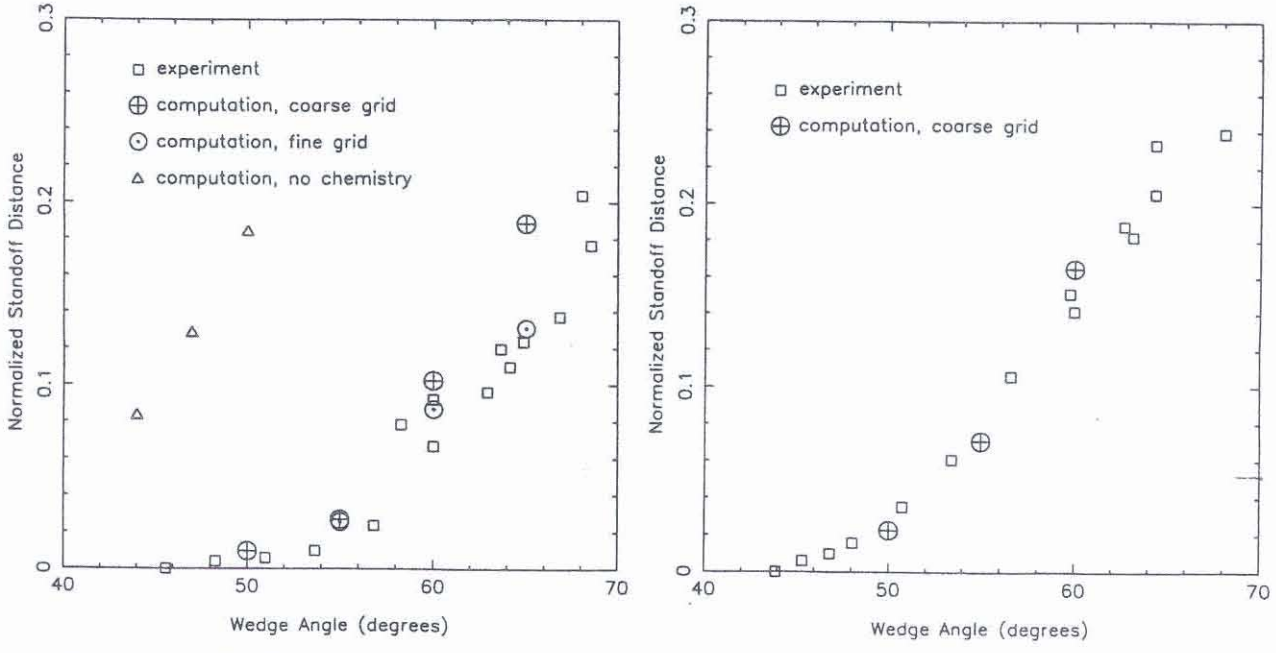

Figure 14 Candler's computation of the flows shown in Figure 10.

a. Temperature field in CO_2 flow over a 65 deg half-angle wedge (fine grid, 110 x 100). Note high temperatures near the shock and in the boundary layer.

b. Carbon dioxide. Note frozen flow points.

c. Comparison of stand-off distance experiment and computation: nitrogen.

(From private communication by Candler)

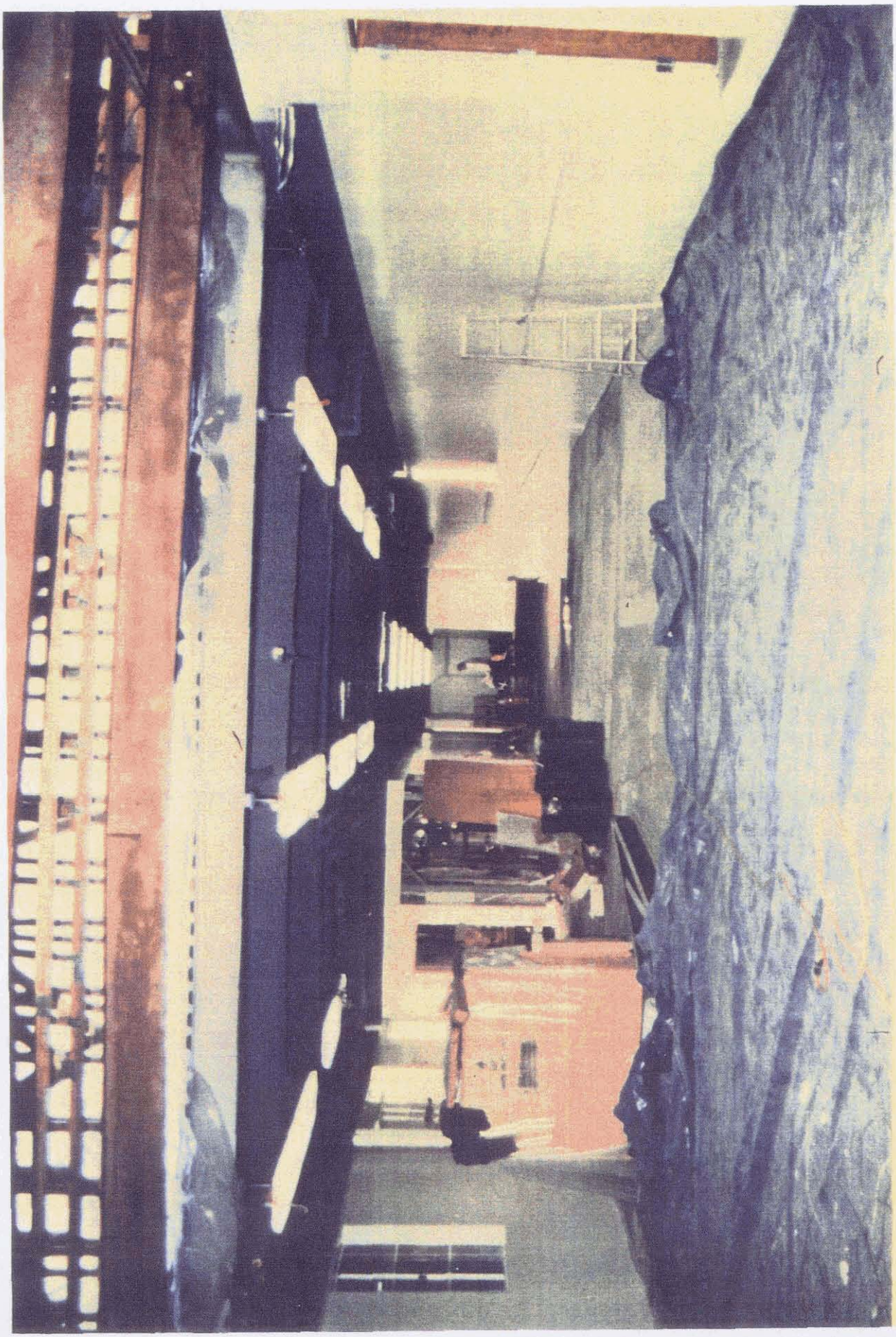

Figure 15 Photograph of the T5 laboratory.

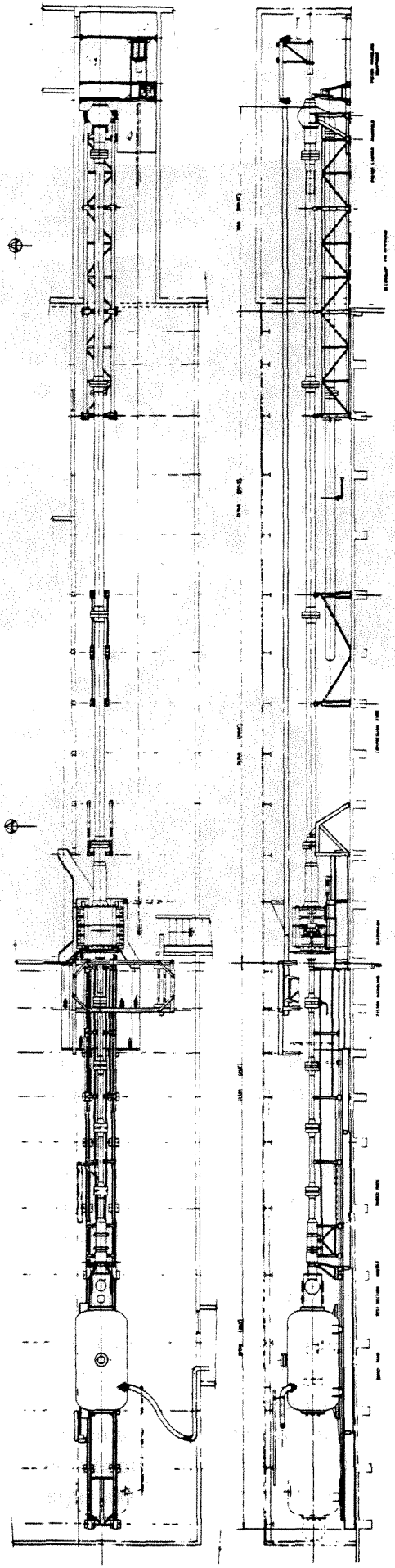

Figure 16 Overall drawing of T5 shock tunnel.

The design of the facility is complete, several parts have been manufactured and are in storage, the remainder are being fabricated by different companies. To give an impression of the magnitude of the task, Table I presents the list of drawings. Figure 16 shows an overall drawing of the facility and a representative photograph of a part is presented in Figure 17.

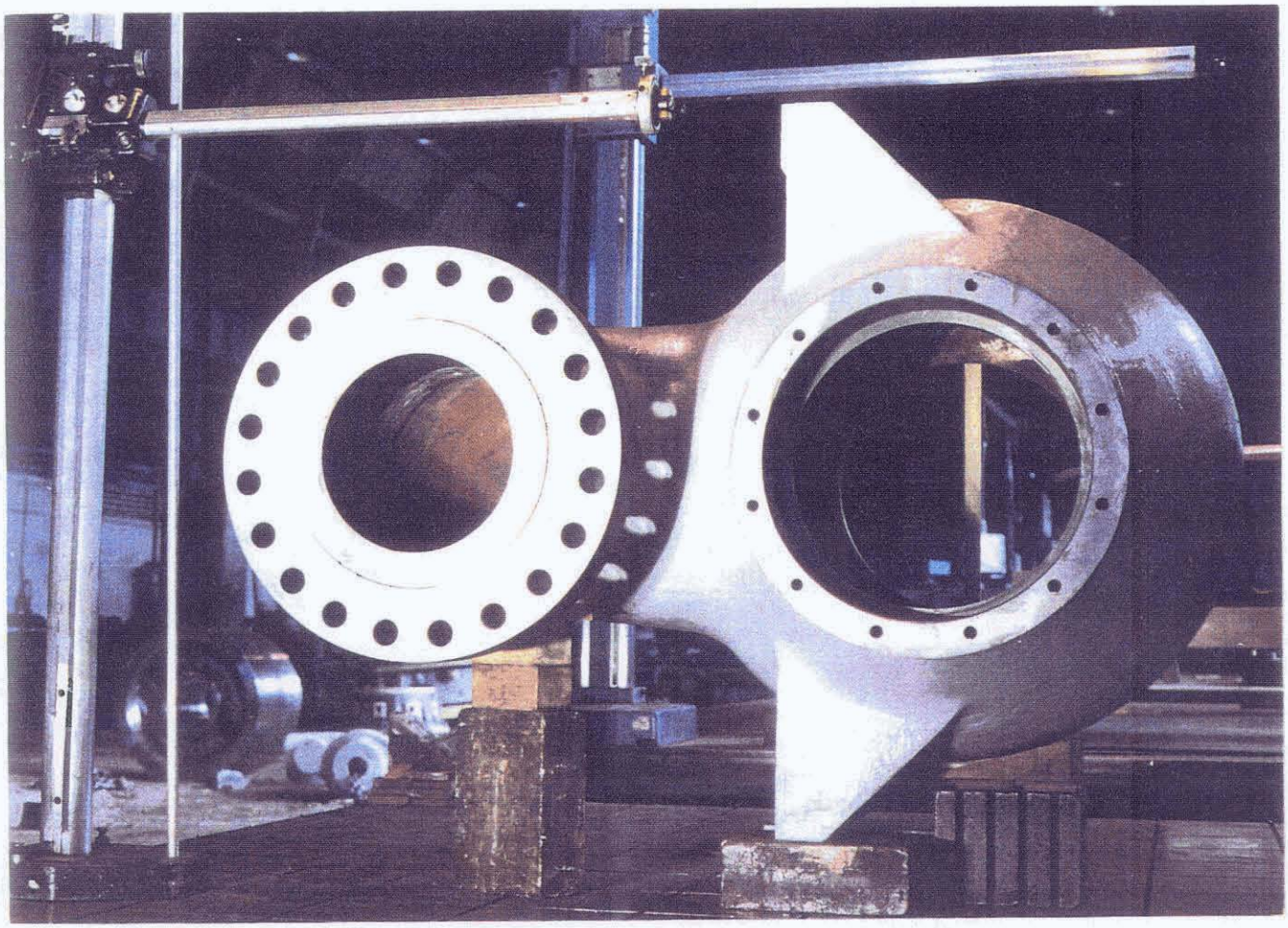

Figure 17 Photograph of launch manifold for T5. This is the part at the extreme right of Figure 16.

The data acquisition system has been selected. Orders are about to be placed. The system provides for 30 channels of digital recording in addition to the channels necessary for the operation and run documentation.

A bare-bones start to an optical diagnostics system consisting of schlieren and interferometry capability has been designed, and orders are about to be placed. Financial constraints presently prohibit the development of a PLIF system. However, discussions with Rocketdyne indicate that it may be possible for us to use the system developed by them for some of our fundamental research projects during a limited period.

None of the gas dynamical calculations necessary for the operation of a high- enthalpy shock tunnel can be done without making fairly sophisticated statistical mechanical computations. To this end, a number of computer codes have been written and tested against existing simpler programs. In particular, a program for inviscid nozzle flow computations in two dimensions and for finite rate chemistry is now operational. This is sufficiently fast and economical to be built into a design loop for optimizing nozzle shape. An example of partial

output of this program for the T5 axisymmetric nozzle is presented in Figure 18.

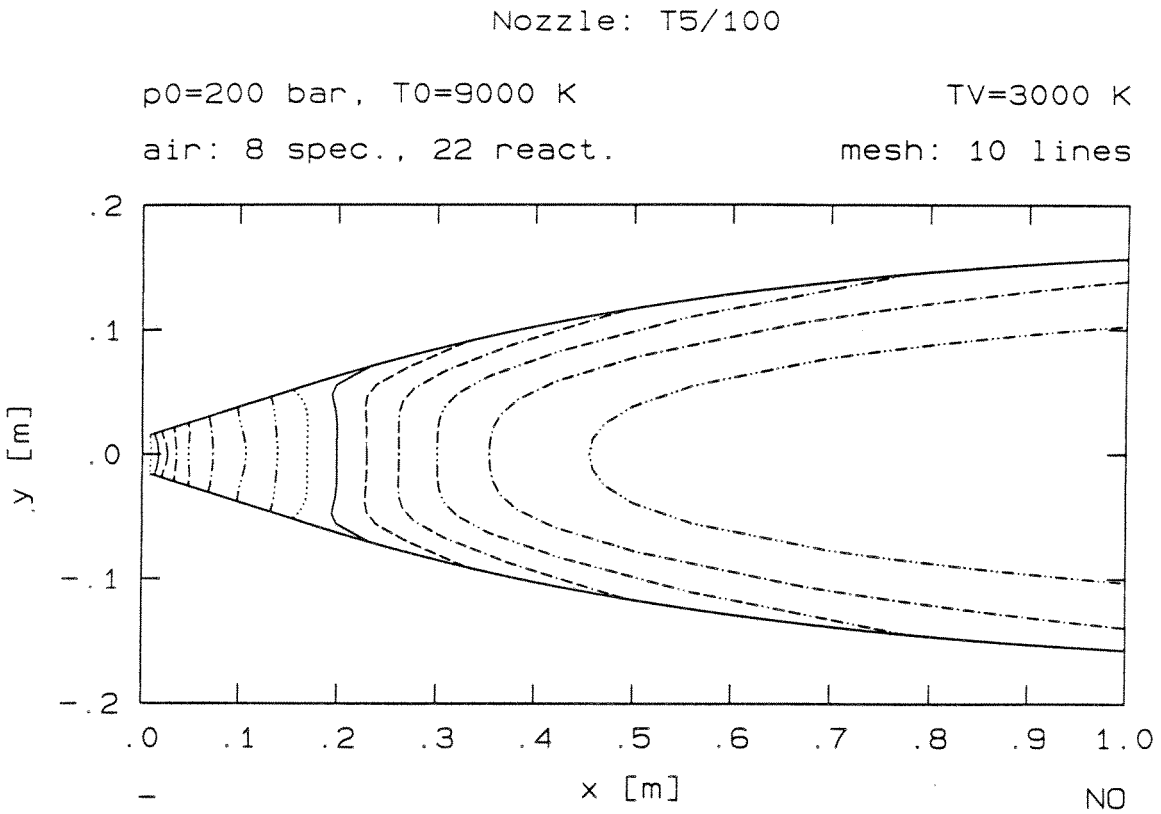

Figure 18 Example of computation of the T5 nozzle (NO concentration contours). (Ref. 10)

5.2 Manpower

The team consists of two faculty members approximately one third of full time, one post-doctoral fellow, three (increasing to five in 1990-1991) graduate students, one technician as well as machine shop and secretarial support. If the facility is operated at a high rate (six shots per 8 hour day is the expected normal rate) a second technician is required. The maximum number of graduate students should probably be 6.

5.3 Relation to industry

Clearly, industrial companies are likely to want to use a nationally unique facility such as T5. Rocketdyne has, of course, already planned to do some tests in the second half of 1990. We welcome such cooperation, not only because it allows us to maintain a dedicated technician, but also because of the very valuable interaction with industry that it provides. This is always stimulating as our interaction over the last 2 1/2 years has amply demonstrated.

5.4 Financial situation and needs

The cost of the facility, including the building is approximately $3.5M. Of this, Rocketdyne has supplied $1.5M from their NASP contract. The remainder will be supplied by Caltech. This very substantial investment on the part of Rocketdyne and Caltech will provide

the means for a step that gives the US its first ground facility to produce high density flows at earth orbital enthalpy. Certainly, there are already plans for others that will follow soon. Not only in the US, but also in West Germany and Japan. However, except for the work proceeding in Australia, we will have a small start in time, and, we believe, also in the location of T5 within a university where the emphasis will be on fundamental progress.

The facility, to the point of primitive operation, can be considered to be funded. The establishment of a proper diagnostics system including PLIF is estimated to cost $450k. An extension of the data acquisition system to 100 channels, and more extensive processing software is estimated to cost $90k. Neither of these two items is presently funded.

The running cost consists mainly of personnel costs and to a lesser degree of expendables. With the average number of 4 paid graduate research fellows and the remainder of the team as outlined above, the running cost is estimated to be $450k per year. At present the research support for FY90 and FY91 is $100k per annum from ONR. This support is limited to these two years as the ONR does not see this field as part of its continuing interest.

It is therefore imperative that we seek funding for the research programs that are proposed in section 3.

6. References

1. Hornung, H. G. Non-equilibrium nitrogen flow over spheres and circular cylinders. *J. Fluid Mech.* 1972, 53, 149-176.
2. Liepmann, H. W. & Roshko, A. *Elements of Gasdynamics*. Wiley, 1957.
3. Morrison, R. To appear in Proceedings, 17th International Symposium on Shock Tubes and Waves, Lehigh, 1989.
4. Hornung, H. G. 28th Lanchester Memorial Lecture - Experimental real-gas hypersonics. Aero. J., December, 1988.
5. Hornung, H. G. Nonequilibrium dissociating flow behind a curved shock wave *J. Fluid Mech.* 1976, 74, 143-160.
6. Ebrahim, N. A. & Hornung, H. G. High-enthalpy non-equilibrium carbon dioxide nozzle and wedge flows *AIAA J.* 1975, 13, 845-846.
7. Hornung, H. G. & Smith, G. H. The influence of relaxation on shock detachment. *J. Fluid Mech.* 1979, 93, 225-239.
8. Hornung, H. G., Oertel, H. & Sandeman, R. J. Transition to Mach reflexion of shock waves in steady and pseudo-steady flow with and without relaxation. *J. Fluid Mech.* 1979, 90, 541-560.
9. Candler, G. On the Computation of Shock Shapes in Nonequilibrium Hypersonic Flows. 27th Aerospace Sciences Meeting, Reno, NV, AIAA-89-0312, 1989
10. Rein, M. Surf: A Program for Calculating Inviscid Supersonic Reacting Flows in Nozzles. GALCIT FM 89-1, California Institute of Technology, 1989.

TABLE I **T5 Drawings and Systems Status**

Dwg.	Primary Title	Secondary Title	Bid Package	System
	Primary Storage Vessels			Primary Vessels
X00-02	**General Arrangement & Design Layout**			General
00-03	**Arrangement**	Sheet 1 of 3		General
00-04	**Arrangement**	Sheet 2 of 3		General
00-05	**Arrangement**	Sheet 3 of 3		General
11-05	**Secondary Air Reservoir**	Assembly		
11-10	**Secondary Air Reservoir**	Front Segment Detail	Secondary Air Reservoir	Secondary Reservoir
11-11	**Secondary Air Reservoir**	End Segment Detail	Secondary Air Reservoir	Secondary Reservoir
X12-02	**Launch Manifold & Secondary Air Reservoir**			Launcher
12-03	**Launch Manifold**	Detail	Launch Manifold	Launcher
12-04	**Launch Manifold**	Bush Detail	Launch Manifold Bushings	Launcher
12-05	**Launch Capsule**	Detail	Lnch Capsl & Breech Comps	Launcher
12-06	**Launch Capsule**	Breech Nut Detail	Lnch Capsl & Breech Comps	Launcher
12-07	**Launch Capsule**	Miscellaneous Details	Lnch Capsl & Breech Comps	Launcher
12-08	**Launch Capsule**	Miscellaneous Details	Lnch Capsl & Breech Comps	Launcher
12-10	**Launch End**	Assembly	Lnch Capsl & Breech Comps	Launcher
13-08	**Compression Tube**	Segment Detail	Compression Tube	Compression Tube
13-09	**Compression Tube**	High Pressure End Detail	CT High Pressure End	Compression Tube
13-10	**Compression Tube**	Inlet & Instrumentation Plate Detail	Instrumentation Plates	Compression Tube
13-11	**Compression Tube**	Launch Segment Detail	Launch Segment	Compression Tube
13-13	**Inertial Mass**	General Arrangement	Inertial Mass Rolling Supports	Inertial Mass
13-14	**Inertial Mass**	Upper Segment	Cast Inertial Mass	Inertial Mass
13-15	**Inertial Mass**	Lower Segment	Cast Inertial Mass	Inertial Mass
13-16	**Inertial Mass**	Upper Segment	Cast Inertial Mass	Inertial Mass
13-17	**Inertial Mass**	Lower Segment	Cast Inertial Mass	Inertial Mass
13-18	**Compression Tube**	Segments & Inlet/Instrumentation Plate Assembly		Compression Tube
13-19	**Inertial Mass**	Roller Support Bracket & Shims	Inertial Mass Rolling Supports	Rolling Support
13-20	**IM, Reservoir, CT, ST**	Stud Details	Extrnlly Thrdd Studs & Rods	Shock Tube
14-01	**CT/ST Connection**	Split Nut Detail	CT/ST Connection Split Nut	Compression Tube
14-02	**CT/ST Connection**	Diaphragm & Piston Buffer Assembly	CT/ST Junction Comp's	Compression Tube
14-03	**CT/ST Connection**	Shock Tube Sleeve Detail	ST Sleeve	Compression Tube
14-04	**CT/ST Connection**	Pressure Plate Detail	CT/ST Junction Comp's	Compression Tube
14-05	**CT/ST Connection**	Component Details	CT/ST Junction Comp's	Compression Tube
14-06	**CT/ST Connection**	Piston Buffer Comp's Details	Piston Buffer	Compression Tube
15-03	**Piston**	Detail	Piston Assembly	Piston
15-04	**Piston**	Seal Detail	Piston Assembly	Piston
15-05	**Piston**	Ring Details	Piston Assembly	Piston
15-06	**Piston**	Brake Details	Piston Assembly	Piston
15-07	**Piston**	Mandrel Details & Assembly	Piston Assembly	Piston
15-08	**Piston**	Assembly	Piston Assembly	Piston
15-09	**Piston**	Special Spanners for Piston Maintenance		
16-03	**Shock Tube**	Segment Detail	ST Segments	Shock Tube
16-04	**Shock Tube**	Instrumentation Plate Detail	Instrumentation Plates	Shock Tube
16-05	**Shock Tube**	Inlet Segment Detail	ST Inlet Segment	Shock Tube
16-06	**Shock Tube**	Inlet & Instrumentation Plate	Instrumentation Plates	Shock Tube
16-07	**Shock Tube**	High Pressure End Detail	ST High Pressure End	Shock Tube
16-08	**Shock Tube**	Segments, Instrument & Inlet Plates Assembly		Shock Tube
16-09	**CT/ST**	Pressure Vents and Adaptor Flanges		
17-01	**ST/Nozzle Connection**	General Arrangement	Nozzle Comp's	Nozzle & Test Section
17-02	**ST/Nozzle Connection**	Nut Detail	CT/ST Connection Split Nut	Shock Tube
17-03	**Nozzle Detail**	Nozzle Comp's		Nozzle & Test Section
17-04	**ST/Nozzle Connection**	Component Details Sh. 1	Nozzle Comp's	Nozzle & Test Section
17-05	**ST/Nozzle Connection**	Component Details Sh. 2	Nozzle Comp's	Nozzle & Test Section
17-06	**ST/Nozzle Connection**	Transducer Plate Detail	Nozzle Comp's	Nozzle & Test Section
17-07	**Nozzle**	Support Detail	Nozzle Comp's	Nozzle & Test Section
18-02	**Test Section**	Arrangement	Test Section	Nozzle & Test Section
18-03	**Test Section**	Details - Sh. 1	Test Section	Nozzle & Test Section
18-04	**Test Section**	Details - Sh. 2	Test Section	Nozzle & Test Section
19-03	**Dump Tank**	Details	Dump Tank	Dump Tank
19-04	**Dump Tank**	Assembly	Dump Tank	Dump Tank

19-05	**Dump Tank**	Drive Assembly	Dump Tank Drive	Handling Systems
19-06	**Dump Tank**	Drive Comp's	Dump Tank Drive	Handling Systems
31-04	**Inertial Mass**	Support Frame Details Sh. 1	Inertial Mass Support Frame	Structural Support
31-05	**Inertial Mass**	Support Frame Details Sh. 2	Inertial Mass Support Frame	Structural Support
31-06	**Inertial Mass**	Support Frame Mounting Pads	Inertial Mass Support Frame	Structural Support
31-07	**Support Roller**	Assembly	CT/ST Rolling Support	Rolling Support
31-08	**Support Roller**	Bracket	CT/ST Rolling Support	Rolling Support
X31-09	**Support Roller**	Details	CT/ST Rolling Support	Rolling Support
31-10	**Compression Tube**	Structural Support Arrangement	Structural Support, CT/LM	Rolling Support
31-11	**ST Handling System**	Assembly	ST Handling System	Handling Systems
31-12	**CT HP End**	Support Structure Details	Structural Support, CT/LM	Structural Support
31-13	**CT/Secondary Res.**	Support Details	Structural Support, CT/LM	Structural Support
31-14	**Compression Tube**	Intermediate Support Details	Structural Support, CT/LM	Structural Support
31-15	**ST Handling System**	Support Frame	ST Handling System	Structural Support
31-16	**ST Handling System**	Support Frame at Nozzle End	ST Handling System	Structural Support
31-17	**ST Handling System**	Tube Drive Clamps	ST Handling System	Structural Support
31-18	**ST Handling System**	Nozzle Support Frame	ST Handling System	Structural Support
31-19	**ST Handling System**	Miscellaneous Details	ST Handling System	Structural Support
31-20	**ST Handling System**	Support Beam	ST Handling System	Structural Support
31-21	**ST Handling System**	Support Beam	ST Handling System	Structural Support
31-22	**ST Handling System**	Support Beam	ST Handling System	Structural Support
31-23	**ST Handling System**	Support Beam	ST Handling System	Structural Support
31-24	**ST Handling System**	Structural Support Details Sh. 1	Structural Support, CT/LM	Structural Support
31-25	**ST Handling System**	Structural Support Details Sh. 2	Structural Support, CT/LM	Structural Support
31-26	**Compression Tube**	Structural Support Positioning Cylinder & Buffers	CT/ST Translation Systems	Handling Systems
31-27	**ST Handling System**	Dump Tank Buffer Support	ST Handling System	Handling Systems
31-28	**ST Handling System**	Splice Plates	ST Handling System	Handling Systems
41-02	**Piston Handling System**	Automatic Piston Latch, Genl Arrngmnt	Automatic Piston Latch	Handling Systems
41-03	**Piston Handling System**	Arrangement, Piston Insertion	Piston Handling/Insertion Sys	Handling Systems
41-04	**Piston Handling System**	Assy & Dtls, Roller Adjstbl Mntng Plates	Piston Extraction System	Handling Systems
41-05	**Piston Handling System**	General Arrangement, Piston Extractor Carriage	Piston Extraction System	Handling Systems
41-06	**Piston Handling System**	Gen'l Arrngmnt, Piston Extractor Supp Structr	Piston Extraction System	Handling Systems
41-07	**Lnch Cpsl Support Carriage**	Assembly	Piston Handling/Insertion Sys	Handling Systems
41-08	**Piston Handling System**	General Arrangement Piston Inspectn Trolley	Piston Handling/Insertion Sys	Handling Systems
41-09	**Lnch Cpsl Insertion Carriage**	Assembly	Piston Handling/Insertion Sys	Handling Systems
41-11	**Piston Handling System**	Details, Piston Extractor Carriage	Piston Extraction System	Handling Systems
41-12	**Piston Handling System**	Piston Extractor Carriage, Misc Dtls	Piston Extraction System	Handling Systems
41-13	**Lnch Cpsl Support Carriage**	Frame Detail	Piston Handling/Insertion Sys	Handling Systems
41-14	**Piston Handling System**	Dtls, Piston Extractor Supp Strctr, Sht 1	Piston Extraction System	Handling Systems
41-15	**Piston Handling System**	Dtls, Piston Extractor Supp Strctr, Sht 2	Piston Extraction System	Handling Systems
41-16	**Piston Handling System**	Dtls, Piston Extractor Supp Strctr, Sht 3	Piston Extraction System	Handling Systems
41-17	**Piston Handling System**	Dtls, Piston Extractor Supp Strctr, Sht 4	Piston Extraction System	Handling Systems
41-18	**Piston Handling System**	Details Piston Inspection Trolley - Sht 1	Piston Handling/Insertion Sys	Handling Systems
41-19	**Lnch Cpsl Insertion Carriage**	Frame Detail	Piston Handling/Insertion Sys	Handling Systems
41-20	**Lnch Cpsl Insertion Carriage**	Mandrel Detail	Piston Handling/Insertion Sys	Handling Systems
41-21	**Lnch Cpsl Insertion Carriage**	Roller Mnting Plates	Piston Handling/Insertion Sys	Handling Systems
41-22	**Lnch Cpsl Support Carriage**	Hinged Support Detail	Piston Handling/Insertion Sys	Handling Systems
41-23	**Piston Handling System**	Piston Inspection Trolley Ltch Dtl	Piston Handling/Insertion Sys	Handling Systems
41-24	**Piston Handling System**	Latch & Suppt Lock Components	Piston Handling/Insertion Sys	Handling Systems
41-25	**Piston Insertion**	Cross Travel Beam & Comps	Piston Handling/Insertion Sys	Handling Systems
41-26	**Piston Handling System**	Cross Travel Frame	Piston Handling/Insertion Sys	Handling Systems
41-27	**Piston Handling System**	Transport Monorail Arrangement	Piston Handling/Insertion Sys	Handling Systems
41-28	**Piston Handling System**	Automatic Piston Latch Details	Automatic Piston Latch	Handling Systems
41-29	**Piston Handling System**	Automatic Piston Latch Details	Automatic Piston Latch	Handling Systems
41-30	**Piston Handling System**	Piston Inspection Trolley Mandrel Detail	Piston Handling/Insertion Sys	Handling Systems
44-02	**CT/ST Translation Systems**	Hydraulic Circuits	CT/ST Translation Systems	Handling Systems
51-01	**Gas Services & Instrumentation**	Schematic		Controls
51-02	**Gas Services & Instrumentation**	Layout: Line Sizes		Controls
52-01	**CT/Secondary Reservoir**	Control Board P1		Controls
52-02	**Shock Tube**	Control Board P2		Controls
52-03	**Dump Tank**	Control Board P3		Controls
52-05	**Location of Limit Switches**	Sheet 1 of 2		Controls
52-06	**Location of Limit Switches**	Sheet 2 of 2		Controls
52-07	**Dump Tank Long Travel**	Power & Control Schematic Diagram		Controls
52-08	**Instrumentation**	Pressure Transducer Mounting Arrangement	Press Transducer Mounting	Controls